Pattern Synthesis of Coupled Antenna Arrays via Element Rotation

J. Ignacio Echeveste, Jesús Rubio, Miguel Á. González de Aza, and Christophe Craeye, *Senior Member, IEEE*

***Abstract*—In this work, a pattern synthesis method is presented for coupled antenna arrays via element rotation. The array is rigorously analyzed with a hybrid and full-wave analysis method based on the 3-D finite element method, modal analysis, generalized scattering matrix, and rotation and translation properties of spherical waves, including mutual coupling effects. The co- and cross-polar components are optimized by means of a gradient method, according to a specific cost function, via successive rotations of the elements.**

***Index Terms*—Array synthesis, element rotation, gradient method, local optimization, mutual coupling, spherical waves.**

I. Introduction

ARRAY synthesis stands for changing any array parameter looking for obtaining some desired characteristics in the array performance. The most common variables changed in the array synthesis are the excitation weights applied to the array elements. Very good results can be obtained in that way, but it has some drawbacks, such as incremented costs or a decrease of the array efficiency. In recent years, position-based synthesis has received increased attention (see [1] and references therein). In the synthesis based on the excitation or the position of the elements, the relationship between the co-(CP) and cross-polar (XP) components is mostly defined by the array element; both variations of the array elements equally affect this ratio.

Element rotation is useful for two different applications. On the one hand, the sidelobe level (SLL) or the XP level can be minimized, while steering the mainbeam in a desired direction with a fixed width. In this sense, a low-sidelobe synthesis via a dipole rotation is proposed in [2] by using genetic algorithms, and a synthesis of planar arrays via element rotation is also presented in [3], which makes use of differential evolution and considers the elements as isolated. On the other hand, an array with circular polarization can be obtained from properly rotated, and phased, linearly polarized elements. Modifications on the radiation pattern can be accomplished with element rotation without increasing the array costs or without decreasing the aperture efficiency. Arrays made up of elements with circular polarization usually have more complex feed chains and losses in the polarizer circuits, if they are fed with more than one excitation port, or they suffer from narrower bandwidth if the circular polarization is accomplished with some modification of the radiators [4]. A well-known alternative is to use sequentially rotated linearly polarized radiating elements [5]. This method has the disadvantages of a poor diagonal plane behavior, a limited bandwidth, and lower gain, compared to an array made of circularly polarized elements [6]. The first two disadvantages are reduced with a randomly rotated array in [4], and the third one can be enhanced as proposed in [7]. Element rotation is also a well-established technique in reflectarray antennas [8].

In this work, a synthesis method for array antennas via element rotation is presented. The array is efficiently analyzed in full-wave form, i.e., involving all the mutual coupling effects. The formulation takes advantage of the spherical-wave representation used in [9], which leads to a strictly analytical treatment of element rotation. The synthesis is carried out with a gradient-based optimization method, originally proposed in [1] for a position-based synthesis of isotropic elements. In [10], a variation of this method is proposed for a position-based synthesis, in which the different embedded element patterns resulting from mutual coupling are analyzed rigorously. Both methods optimize the positions of the elements, while the present method looks for optimizing the rotation angle of the elements. The rigorous expression of the radiation intensity of the coupled array is part of the cost function, and its gradient w.r.t. the elements rotation is efficiently obtained, as it is computed analytically.

II. Analysis of the Coupled Array

A rigorous characterization of the coupled array is accomplished with the method proposed in [9]. This technique computes the generalized scattering matrix (GSM) of each element of the array as an isolated antenna with a hybrid method that combines modal analysis, the finite element method, and the domain decomposition technique. Then, the GSM of the coupled array is computed from the GSMs of the isolated antennas using the properties of rotation and translation of spherical waves. A column vector of complex coefficients of the scattered spherical modes, $\boldsymbol{b}$, is computed from the column vector of the complex coefficients of the excitation weights applied to the array elements, $\boldsymbol{v}$, as $\boldsymbol{b} = \boldsymbol{T}_G \boldsymbol{v}$. $\boldsymbol{T}_G$ is the transmission matrix of the coupled array when there is no rotation of the elements and is obtained as shown in [9]

$$\boldsymbol{T}_G = [\boldsymbol{I} - (\boldsymbol{S} - \boldsymbol{I})\boldsymbol{G}]^{-1}\boldsymbol{T} \tag{1}$$

Manuscript received December 23, 2016; accepted February 8, 2017. Date of publication February 13, 2017; date of current version June 19, 2017. This work was supported by MINECO, Spain, under Contracts TEC2013-46282-C2-1-P and TEC2013-46282-C2-2P and by FEDER (EU).

J. Ignacio Echeveste and C. Craeye are with the ICTEAM Institute, Université catholique de Louvain, 1348 Louvain-la-Neuve, Belgium (e-mail: jose.echeveste@uclouvain.be; christophe.craeye@uclouvain.be).

J. Rubio is with the Departamento de Tecnología de Computadores y Comunicaciones, Escuela Politécnica de Cáceres, Universidad de Extremadura, 10071 Cáceres, Spain (e-mail: jesusrubio@unex.es).

M. A. González de Aza is with the Departamento de Señales, Sistemas y Radiocomunicaciones, E.T.S.I. Telecomunicación, Universidad Politécnica de Madrid, 28040 Madrid, Spain (e-mail: mag@etc.upm.es).

Color versions of one or more of the figures in this letter are available online at http://ieeexplore.ieee.org.

Digital Object Identifier 10.1109/LAWP.2017.2668397

where $\boldsymbol{S}$ and $\boldsymbol{T}$ are diagonal matrices, respectively, including the scattering and transmission matrices of the isolated elements of the array on their main diagonals. $\boldsymbol{I}$ is the identity matrix, and $\boldsymbol{G}$ is the general translation matrix as defined in [9].

The transmission matrix of the array when there is a given rotation in the φ-angle between elements is computed as

$$\boldsymbol{T}_{G_F} = [\boldsymbol{I} - (\boldsymbol{S} - \boldsymbol{I})\boldsymbol{G}_F]^{-1}\boldsymbol{T} \tag{2}$$

where $\boldsymbol{G}_F$ is the general translation matrix of the array accounting for this rotation. This matrix is computed as $\boldsymbol{G}_F = \boldsymbol{F}^H\boldsymbol{G}\boldsymbol{F}$, where $\boldsymbol{F}$ is a diagonal matrix whose nonzero entries are given by $F_{ii} = e^{-jm_s\Phi_i}$, where m_s is the order of the spherical wave function and Φ_i is the rotation angle for antenna i. With a variation of the process followed in [9] for accounting for the rotation of the elements, considering a planar array of M antennas on the xy-plane and Q spherical modes in each antenna, given by the row vector $\boldsymbol{e} = (\boldsymbol{e}_1, \boldsymbol{e}_2, \dots \boldsymbol{e}_Q)$ containing the electric fields of these modes, the radiated field is obtained applying superposition as

$$\boldsymbol{E}(\hat{u}) = (\boldsymbol{e}(\hat{u})\, e^{jk\hat{u}\cdot\boldsymbol{u}})\boldsymbol{F}\,\boldsymbol{T}_{G_F}\,\boldsymbol{v} \tag{3}$$

where $(\boldsymbol{e}(\hat{u})\, e^{jk\hat{u}\cdot\boldsymbol{u}}) = (\boldsymbol{e}\, e^{jk\hat{u}\cdot\boldsymbol{u}_1}, \boldsymbol{e}\, e^{jk\hat{u}\cdot\boldsymbol{u}_2}, \dots, \boldsymbol{e}\, e^{jk\hat{u}\cdot\boldsymbol{u}_N})$. k is the wavenumber in free space, $\hat{u}$ is the unitary vector in spherical coordinates, and $\boldsymbol{u}_i$ is the position vector of antenna i, $\boldsymbol{u}_i = x_i\hat{x} + y_i\hat{y}$. The resulting expression is valid for arrays with arbitrary spatial distributions and Φ rotations.

III. Proposed Synthesis Method

In this section, a synthesis method for coupled arrays, characterized by expression (3), is developed. Starting from an initial configuration, a local and gradient-based optimization is established, in which some desired characteristics, represented by a cost function, are iteratively pursued.

The proposed radiation pattern synthesis method aims at fixing a mainbeam with a desired width, while minimizing the SLL and the XP component. This is accomplished with successive rotations of the elements. Two cost functions, built up from the radiation intensity, are defined to separately deal with the CP and XP components. Instead of looking for an average value of the radiation intensity in every direction, a weighting function, $W(\hat{u})$, is introduced in order to impose distinct specifications for different radiation sectors. Consequently, different weighting functions are defined for the CP and XP components and one looks for minimizing them in desired directions, based on an L_p-norm defined in [1]

$$CF_\chi = \left(\int_U \left[W_\chi(\hat{u}) |\boldsymbol{E}_\chi(\hat{u})|^2 \right]^p d\hat{u} \right)^{1/p} \tag{4}$$

where χ now stands for CP or XP. The global cost function is then obtained as a linear combination of both cost functions.

It is interesting to notice that the expression of the cost function is differentiable w.r.t. the element rotation angle Φ. A local and gradient-based optimization method, similar to the one developed in [1] for aperiodic arrays of isotropic elements, is performed here for coupled arrays where the elements pattern and the mutual coupling between them are rigorously taken into account. First, the cost function is computed for an initial configuration; the gradient w.r.t. the element rotation of the cost function is then computed, and the elements are rotated iteratively along the partial gradient multiplied by a constant step $\Delta\Phi$.

The cost function for the coupled antenna array is obtained by substituting into (4) the radiation intensity of the coupled antenna array, which is obtained directly from the expression of the radiated field (3), yielding

$$\begin{aligned} |\boldsymbol{E}(\hat{u})|^2 &= \boldsymbol{v}^H \boldsymbol{T}_{G_F}^H \boldsymbol{F}^H (\boldsymbol{e}(\hat{u}) e^{jk\hat{u}\cdot\boldsymbol{u}})^H \cdot (\boldsymbol{e}(\hat{u}) e^{jk\hat{u}\cdot\boldsymbol{u}}) \boldsymbol{F}\boldsymbol{T}_{\boldsymbol{G_F}}\boldsymbol{v} \\ &= \boldsymbol{v}^H \boldsymbol{P}\boldsymbol{v} \end{aligned} \tag{5}$$

where $\cdot$ stands for the dot product and the superscript H for the Hermitian transpose.

The gradient of the cost function versus the rotation angle of each element of the array is obtained as follows:

$$\frac{\partial CF_\chi}{\partial \Phi_i} = (CF_\chi)^{1-p} \int_u W_\chi(\hat{u})^p \left[\boldsymbol{v}^H \boldsymbol{P}_\chi \boldsymbol{v}\right]^{p-1} \frac{\partial (\boldsymbol{v}^H \boldsymbol{P}_\chi \boldsymbol{v})}{\partial \Phi_i} d\hat{u}. \tag{6}$$

The derivative of the radiation intensity in (6) is computed as

$$\begin{aligned} \frac{\partial |\boldsymbol{E}_\chi(\hat{u})|^2}{\partial \Phi_i} &= \frac{\partial (\boldsymbol{v}^H \boldsymbol{P}_\chi \boldsymbol{v})}{\partial \Phi_i} = \boldsymbol{v}^H \frac{\partial \boldsymbol{P}_\chi}{\partial \Phi_i} \boldsymbol{v} = \\ \boldsymbol{v}^H & \frac{\partial \left[\boldsymbol{F}^H \boldsymbol{T}_{G_F}^H (\boldsymbol{e}_\chi(\hat{u})\, e^{jk\hat{u}\cdot\boldsymbol{u}}) \cdot (\boldsymbol{e}_\chi(\hat{u})\, e^{jk\hat{u}\cdot\boldsymbol{u}})^T \boldsymbol{T}_{G_F} \boldsymbol{F} \right]}{\partial \Phi_i} \boldsymbol{v}. \end{aligned} \tag{7}$$

The transmission matrix of the finite array, $\boldsymbol{T}_{G_F}$, which has been previously defined in (2), can be rewritten for simplicity as $\boldsymbol{T}_{G_F} = \boldsymbol{M}^{-1}\boldsymbol{T}$, where $\boldsymbol{M} = \left[\boldsymbol{I} - (\boldsymbol{S} - \boldsymbol{I})\boldsymbol{G}_F\right]$ is the only Φ-dependent factor. The gradient of the transmission matrix is computed as

$$\frac{\partial \boldsymbol{T}_{G_F}}{\partial \Phi_i} = \boldsymbol{M}^{-1} (\boldsymbol{S} - \boldsymbol{I})\, \frac{\partial \boldsymbol{G}_F}{\partial \Phi_i} \boldsymbol{M}^{-1}\boldsymbol{T} \tag{8}$$

where $\partial \boldsymbol{G}_F / \partial \Phi_i$ is obtained applying the chain rule.

The initial configurations used in this work are arrays with uniformly aligned elements for linear polarization, or sequentially rotated arrays for circular polarization. The optimized result and the convergence will depend on the starting point. A phase variation is needed to obtain the circular polarization from linearly polarized elements. In [5], the angle of rotation of the elements is also employed as the excitation phase. In this work, the excitation phase is determined following the rotation angle, and thus, it has to be considered in the gradient computation. The excitation phase appears through a complex exponential factor, and it is directly derived in the cost function using the chain rule. Steered beams can also be designed. The steering angle will affect the synthesized rotations. In the case of circular polarization, the phase applied to the array elements is computed as the result of the contribution from the phase accounting for the rotation and the phase needed to steer the beam, yielding [4]: $\Phi = \Phi_{\text{rot}} + \Phi_{\text{ste}}$.

IV. Results

A. Linear Array With Linear Polarization of Square and Cavity-Backed Patch Antennas

In the first example, an E-plane linear array made of 14 coaxial probe-fed and cavity-backed square patch antennas is synthesized. The radiating elements are uniformly excited and regularly placed at a distance of $0.6\lambda_0$ at their resonance frequency of 6.1 GHz. The geometry of the radiating element is

TABLE I
SYNTHESIZED ROTATION ANGLES ($\Phi_{\rm rot}$ IN DEGREES) OF THE 14-ELEMENT LINEAR ARRAY OF PATCHES IN THE FIRST EXAMPLE (SEE SECTION IV-A)

N.	1	2	3	4	5	6	7
$\Phi_{\rm rot}$	2.3	13.6	7.3	12.2	−0.4	−7.8	−0.5
N.	8	9	10	11	12	13	14
$\Phi_{\rm rot}$	5.1	−3.9	3.6	−20.4	48.1	−51.3	14.8

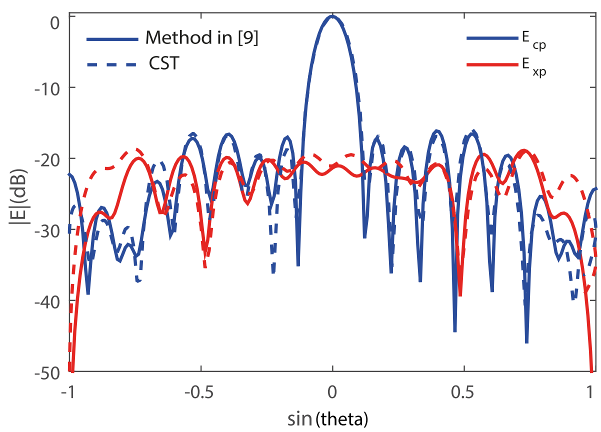

Fig. 1. Comparison of the synthesized array between the one obtained with the method proposed in [9] and the simulated with CST.

obtained from [9]. The objective is to minimize the SLL defined for $|u| \geq 0.13$, keeping a constant mainbeam width and controlling the XP level at acceptable values. The weighting functions applied to the CP and XP components are, respectively

$$W_{\rm cp} = \left[1 - \sin\left(\frac{(\beta - \frac{1+R_i}{2})\pi}{1-R_i}\right)\right]\frac{1}{\beta^q} \qquad W_{\rm xp} = 1 - \beta^2 \qquad (9)$$

where R_i is the radius that defines the sidelobe region, β is the norm of the vector (u_x, u_y) defined as $\beta = (u_x^2 + u_y^2)^{1/2}$, and q allows a softer or sharper variation of W, as explained in [1]. For this example, $q = 0.5$ and $p = 6$ in (4) have been selected. The weighting function of the CP component, $W_{\rm cp}$, gives more importance to the secondary lobes that are close to the mainbeam, while the weighting function of the XP component, $W_{\rm xp}$, focuses on the direction of the mainbeam.

The synthesized angles of rotation are detailed in Table I. Fig. 1 represents the CP and XP components of the electric field. While the unrotated array has the common SLL of −13.3 dB, the maximum CP level is minimized to −16.1 dB in the sidelobe region with the synthesized rotations. The maximum XP component is lower than −18.9 dB. In this example, a considerable reduction in the SLL is accomplished without increasing the fabrication cost, at the expense of a slightly higher XP level. For validation purposes, the resulting synthesis is simulated with the commercial software CST MS. As shown in Fig. 1, they compare very well for the CP and XP components. Differences in angles between 0.8 and 1 can be observed due to the effect of the finite size of the ground plane considered in the CST simulation.

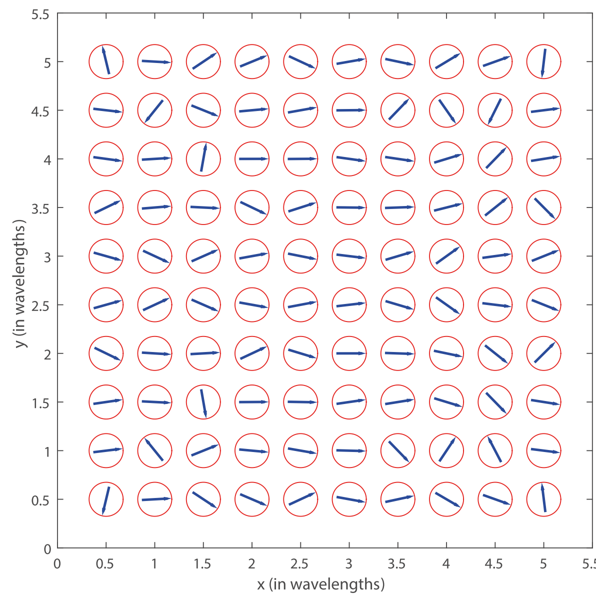

Fig. 2. Representation of the synthesized rotations of the linearly polarized array made of 10×10 HDRAs in the second example (see Section IV-B).

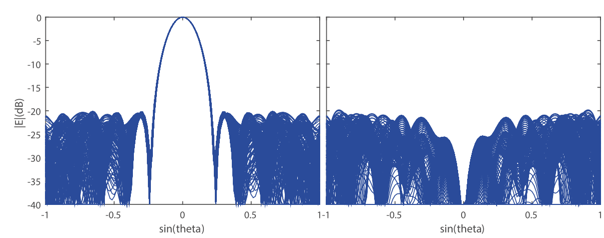

(a) (b)

Fig. 3. 360 phi-cuts of the (a) CP and (b) XP components of the radiation pattern of the synthesized array made of 10×10 HDRAs.

B. Planar Array With Linear Polarization of Hemispherical Dielectric Resonator Antennas

In this second example, a linearly polarized planar array of 10×10 hemispherical dielectric resonator antennas (HDRAs) is synthesized. The geometry of the array element is obtained from [11]. The elements are also uniformly excited and are regularly placed with an interelement distance of $0.5\lambda_0$ at the resonance frequency of 3.64 GHz. The rotation angles are optimized looking for a broadside pattern minimizing the SLL, defined for $|\boldsymbol{u}| \geq 0.2$, and the maximum XP level. In this example, $q = 0.5$ and $p = 8$ are selected. A uniform weighting function ($W = 1$) is used for the CP and XP components, looking for a similar performance in both of them. The starting point is the nonrotated array. The synthesized rotation angles are represented in Fig. 2. The resulting CP and XP radiation patterns are shown in Fig. 3(a) and (b), respectively. As observed, a maximum SLL and XP level of, respectively, −20.1 and −19.9 dB are achieved. Compared to the nonrotated array, the SLL has been decreased by almost 7 dB, while the XP component has been slightly increased. Mutual coupling plays an important role and must be taken into account, especially for elements with a high level of mutual coupling, such as the dielectric resonator antenna of the present example, with a coupling level of the order of −15 dB between contiguous elements. In order to illustrate the coupling effect, the synthesis has been carried out with noncoupled array

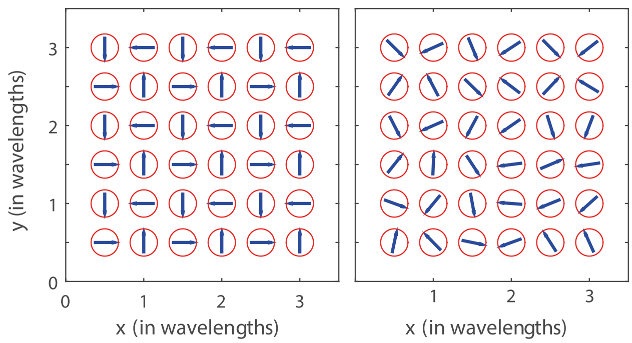

(a) (b)

Fig. 4. (a) 6×6 sequentially rotated elements used as an initial configuration in the last example (see Section IV-C). (b) Synthesized rotations.

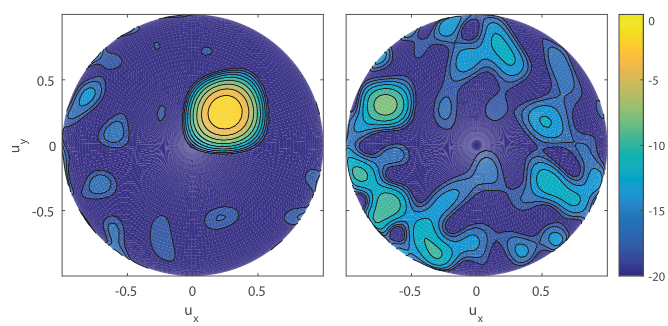

(a) (b)

Fig. 5. (a) CP and (b) XP components of the radiation pattern of the synthesized array of the 6×6 array of HDRAs in the last example (see Section IV-C).

elements, and the synthesized rotation angles have been applied to the coupled array. The resulting radiation pattern shows higher maximum SLL and XP level of -15.5 and -14.5 dB, respectively (to be compared to -20.1 and -19.9 dB).

C. Planar Array With Circular Polarization Made of Hemispherical Dielectric Resonator Antennas

In this last example, a circularly polarized planar array is obtained from linearly polarized elements. The array is composed of 6×6 antennas, and the radiating element is the same as in the previous example. The phase of the elements in this case is obtained as explained at the end of Section III.

The mainbeam is steered toward $u_{x0} = u_{y0} = 0.24$. A phase needed to steer the beam is obtained, as in classical theory: $\Phi_{\text{ste}} = k\hat{u}\boldsymbol{u}_i$. The weighting functions used in this example are the same as in the example of Section IV-A, with $\beta^2 = (u_x - u_{x0})^2 + (u_y - u_{y0})^2$. The initial sequentially rotated array is shown in Fig. 4(a), while the synthesized array is represented in Fig. 4(b). The CP component of the sequentially rotated array has a maximum SLL of -6.5 dB, while the synthesized array, represented in Fig. 5(a), obtains an SLL of -13 dB. The XP component level of the sequentially rotated array is -9.5 dB in the direction of the mainbeam and has a maximum level of -2.7 dB. The XP component level of the synthesized array, represented in Fig. 5(b), has a level of -17 dB in the mainbeam direction and a maximum level of -7.5 dB in the sidelobe region.

TABLE II
Time Required for the Analysis of the Element (Elem.) and for the Coupled Array (Array); Number of Iterations of the Synthesis (No. it.), Time in the Optimization Process (Opt.), and Number of Variables of Optimization (No. Var.)

Example	Analysis (s)		Synthesis		No. Var.
	Elem.	Array	No. It.	Opt. (min)	
Lin. array	15	1	37	0.75	14
Plan. LP array	20	4	25	57	100
Plan. CP array	20	3	21	31	36

Table II shows the number of variables, the number of iterations, and the time required for the analysis and synthesis for the three examples shown in this work.

V. Conclusion

An array synthesis approach has been presented including mutual coupling for antenna arrays via element rotation, based on a gradient method where derivatives are analytically calculated. A rigorous expression of the radiation intensity is obtained and integrated in a cost function. The gradient of the cost function is efficiently obtained w.r.t. the elements rotation, and the cost function is minimized with iterative rotations of the elements. In this way, a highly nonconvex problem is solved very efficiently, providing high-performance arrays with realistic elements.

References

[1] T. Clavier *et al.*, "A global-local synthesis approach for large non-regular arrays," *IEEE Trans. Antennas Propag.*, vol. 62, no. 4, pp. 1596–1606, Apr. 2014.

[2] R. L. Haupt and D. Aten, "Low sidelobe arrays via dipole rotation," *IEEE Trans. Antennas Propag.*, vol. 57, no. 5, pp. 1575–1579, May 2009.

[3] F. Zhang, F.-S. Zhang, C. Lin, G. Zhao, and Y.-C. Jiao, "Pattern synthesis for planar array based on elements rotation," *Prog. Electromagn. Res. Lett.*, vol. 11, pp. 55–64, 2009.

[4] A. Smolders and H. Visser, "Low side-lobe circularly-polarized phased arrays using a random sequential rotation technique," *IEEE Trans. Antennas Propag.*, vol. 62, no. 12, pp. 6476–6481, Dec. 2014.

[5] J. Huang, "A technique for an array to generate circular polarization with linearly polarized elements," *IEEE Trans. Antennas Propag.*, vol. AP-34, no. 9, pp. 1113–1124, Sep. 1986.

[6] A. Bhattacharyya, "Comparison between arrays of rotating linearly polarized elements and circularly polarized elements," *IEEE Trans. Antennas Propag.*, vol. 56, no. 9, pp. 2949–2954, Sep. 2008.

[7] H. Iwasaki, T. Nakajima, and Y. Suzuki, "Gain improvement of circularly polarized array antenna using linearly polarized elements," *IEEE Trans. Antennas Propag.*, vol. 43, no. 6, pp. 604–608, Jun. 1995.

[8] J. Huang and R. Pogorzelski, "A ka-band microstrip reflectarray with elements having variable rotation angles," *IEEE Trans. Antennas Propag.*, vol. 46, no. 5, pp. 650–656, May 1998.

[9] J. Rubio, M. Á. González de Aza, and J. Zapata, "Generalized-scattering-matrix analysis of a class of finite arrays of coupled antennas by using 3-D FEM and spherical mode expansion," *IEEE Trans. Antennas Propag.*, vol. 53, no. 3, pp. 1133–1144, Mar. 2005.

[10] J. I. Echeveste, J. Rubio, M. Á. González de Aza, and C. Craeye, "Gradient-based aperiodic array synthesis of real arrays with uniform amplitude excitation including mutual coupling," *IEEE Trans. Antennas Propag.*, vol. 65, no. 2, pp. 541–551, Feb. 2017.

[11] K. Leung, K. Luk, K. Y. A. Lai, and D. Lin, "Theory and experiment of a coaxial probe fed hemispherical dielectric resonator antenna," *IEEE Trans. Antennas Propag.*, vol. 41, no. 10, pp. 1390–1398, Oct. 1993.